Two-point optical coherency matrix tomography

Ayman F. Abouraddy,* Kumel H. Kagalwala, and Bahaa E. A. Saleh

CREOL, The College of Optics & Photonics, University of Central Florida, Orlando, Florida 32816, USA

**Corresponding author: raddy@creol.ucf.edu*

Received February 10, 2014; accepted March 12, 2014;
posted March 13, 2014 (Doc. ID 206195); published April 10, 2014

The two-point coherence of an electromagnetic field is represented completely by a 4×4 coherency matrix **G** that encodes the joint polarization–spatial-field correlations. Here, we describe a systematic sequence of cascaded spatial and polarization projective measurements that are sufficient to tomographically reconstruct **G**—a task that, to the best of our knowledge, has not yet been realized. Our approach benefits from the correspondence between this reconstruction problem in *classical* optics and that of quantum state tomography for two-photon states in *quantum* optics. Identifying **G** uniquely determines all the measurable correlation characteristics of the field and, thus, lifts ambiguities that arise from reliance on traditional scalar descriptors, especially when the field's degrees of freedom are correlated or classically entangled.

OCIS codes: (030.1640) Coherence; (260.5430) Polarization; (120.3180) Interferometry; (030.6600) Statistical optics.
http://dx.doi.org/10.1364/OL.39.002411

The concepts of partial polarization at a point in an optical field and partial spatial coherence in a scalar field are both well understood [1]. Partially coherent electromagnetic fields, in which both of these aspects are inextricably linked, have received considerable attention over the past decade or so [2–5]. It is well-established that the coherence of an electromagnetic field [6] (quantified by two-point field correlations) is represented by a 4×4 coherency matrix **G** [7]. This matrix is a *complete* representation of *second-order field correlations* (first-order coherence) for any two points in the field. Therefore, *all* proposed measures of vector-field coherence are in fact scalar functions of the elements of **G** [3,4]. Furthermore, the importance of **G** stems from its predictive power: it determines the coherence properties after any subsequent linear manipulation of the field at these two points.

Despite its fundamental importance, the elements of **G** have *not* been directly measured in their entirety, heretofore, and proposed approaches to achieving this goal are lacking. Here, we present a systematic measurement methodology to reconstruct **G** for an electromagnetic field. Moreover, this approach is applicable to any two (or more) discrete degrees of freedom (DOFs) of an optical field. Underpinning this strategy is a finite set of optical measurements (following appropriate field transformations and projections) that may be inverted to yield the complex elements of **G**. The choice of the particular measurements to be implemented is elucidated by highlighting the correspondence between the problem of identifying the elements of **G** in *classical* optics and identifying the complex elements of the density matrix associated with two-photon states in *quantum* optics —a process typically known as quantum state tomography [8,9]. In light of this correspondence, we call the approach described here *optical coherency matrix tomography*, applied in the current context to the particular case of two-point polarization correlations.

We first consider the polarization DOF at a single point in a *quasi-monochromatic* beam, which is represented by a 2×2 Hermitian polarization coherency matrix:

$$\mathbf{G}_{\mathrm{p}} = \begin{pmatrix} G_{\mathrm{HH}} & G_{\mathrm{HV}} \\ G_{\mathrm{VH}} & G_{\mathrm{VV}} \end{pmatrix} = \frac{1}{2}\sum_{\ell=0}^{3} S_{\ell}^{\mathrm{p}} \hat{\sigma}_{\ell} = \frac{1}{2}\begin{pmatrix} S_0^{\mathrm{p}} + S_1^{\mathrm{p}} & S_2^{\mathrm{p}} - iS_3^{\mathrm{p}} \\ S_2^{\mathrm{p}} + iS_3^{\mathrm{p}} & S_0^{\mathrm{p}} - S_1^{\mathrm{p}} \end{pmatrix}, \tag{1}$$

where $G_{jj'} = \langle E_j(\vec{r}) E_{j'}^*(\vec{r}) \rangle$, $G_{jj'} = G_{j'j}^*$, $E_j(\vec{r})$ is the H or V field component at $\vec{r}$, $\{S_{\ell}^{\mathrm{p}}\}$ are the Stokes parameters, and $\hat{\sigma}_{\ell}$ ($\ell = 0 \ldots 3$) are the Pauli matrices defined as

$$\hat{\sigma}_0 = \begin{pmatrix} 1 & 0 \\ 0 & 1 \end{pmatrix}, \quad \hat{\sigma}_1 = \begin{pmatrix} 1 & 0 \\ 0 & -1 \end{pmatrix},$$
$$\hat{\sigma}_2 = \begin{pmatrix} 0 & 1 \\ 1 & 0 \end{pmatrix}, \quad \hat{\sigma}_3 = \begin{pmatrix} 0 & -i \\ i & 0 \end{pmatrix}.$$

The degree of polarization D_{p} is defined as $D_{\mathrm{p}} = (1/S_0^{\mathrm{p}})\sqrt{(S_1^{\mathrm{p}})^2 + (S_2^{\mathrm{p}})^2 + (S_3^{\mathrm{p}})^2}$. This representation contains four real parameters that may be identified experimentally via the four polarization projections shown in Fig. 1(a): the total power I_0 and that of the H, 45°, and right-hand circular (RHC) polarization components, corresponding to I_1, I_2, and I_3, respectively. These measurements yield the Stokes parameters since $S_j^{\mathrm{p}} = 2I_j - I_0$, $j = 0 \ldots 3$. Note that normalizing the measurements with respect to I_0 yields a unity-trace $\mathbf{G}_{\mathrm{p}}$, which is now in one-to-one correspondence with the density operator used in quantum optics to describe one-photon polarization states [10,11], or, more generally, any two-level quantum system.

Such a formalism may also be used to capture the two-point *spatial* correlations in a *scalar* field. The corresponding representation of spatial coherence using two-point correlations at $\vec{r}_{\mathrm{a}}$ and $\vec{r}_{\mathrm{b}}$ is a spatial

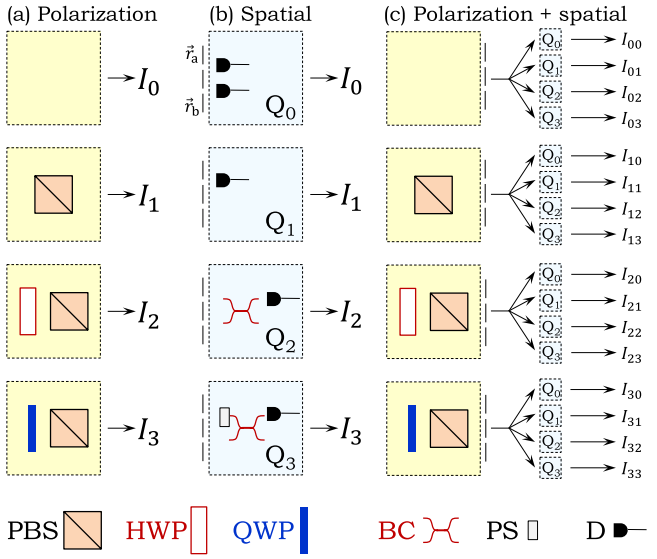

Fig. 1. (a) Projective measurements to reconstruct $\mathbf{G}_\mathrm{p}$. PBS, polarizing beam splitter; HWP, half-wave plate to rotate polarization by 45°; QWP, quarter-wave plate that transforms H to RHC polarization. The empty box corresponds to measuring the total power. (b) projective measurements to reconstruct $\mathbf{G}_\mathrm{s}$ at $\vec{r}_\mathrm{a}$ and $\vec{r}_\mathrm{b}$. BC, symmetric beam combiner; PS, a $\pi/2$ phase shifter; D, detector. All components in (b) are polarization *in*sensitive. (c) Sixteen projective measurements to reconstruct $\mathbf{G}$ for a vector field at $\vec{r}_\mathrm{a}$ and $\vec{r}_\mathrm{b}$ constructed by cascading measurements from (a) and (b).

coherency matrix, $\mathbf{G}_\mathrm{s} = \left(\begin{smallmatrix} G_\mathrm{aa} & G_\mathrm{ab} \\ G_\mathrm{ba} & G_\mathrm{bb} \end{smallmatrix}\right) = (1/2)\sum_{m=0}^{3} S_m^\mathrm{s}\hat{\sigma}_m$, where $G_{kk'} = \langle E(\vec{r}_k)E^*(\vec{r}_{k'})\rangle$, $G_{kk'} = G_{k'k}^*$, $k,k' = \mathrm{a},\mathrm{b}$, and $\{S_m^\mathrm{s}\}$ are two-point *spatial* Stokes parameters. The elements of $\mathbf{G}_\mathrm{s}$ may be obtained experimentally using the spatial projective measurements shown in Fig. 1(b) *without* recourse to recording spatial interference patterns: the total power I_0; the power I_1 at one position, e.g., $\vec{r}_\mathrm{a}$ (corresponding to the H-polarization measurement above); the power I_2 after symmetric mixing of the field at $\vec{r}_\mathrm{a}$ and $\vec{r}_\mathrm{b}$ (corresponding to the 45°-polarization measurement); and I_3 obtained similarly to I_2 except for a $\pi/2$ phase shift placed at $\vec{r}_\mathrm{b}$ (corresponding to the RHC-polarization measurement). As with the case of polarization above, $\mathbf{G}_\mathrm{s}$ is normalized such that $S_0^\mathrm{s} = 1$ puts $\mathbf{G}_\mathrm{s}$ in one-to-one correspondence with density operators that describe two-level quantum systems. The visibility of Young's interferogram produced by the field at these two points is then simply $V = 2|\Re\{G_\mathrm{ab}\}| = |S_2^\mathrm{s}|$, which is clearly not sufficient to retrieve all the parameters of $\mathbf{G}_\mathrm{s}$. In analogy to D_p, we define a spatial counterpart of the degree of polarization as the degree of spatial coherence $D_\mathrm{s} = (1/S_0^\mathrm{s})\sqrt{(S_1^\mathrm{s})^2 + (S_2^\mathrm{s})^2 + (S_3^\mathrm{s})^2}$. This quantity has a clear interpretation: it is the *maximum* observable visibility from the field at $\vec{r}_\mathrm{a}$ and $\vec{r}_\mathrm{b}$ after an arbitrary unitary transformation is implemented. That is, after inserting relative phases and/or mixing the field from $\vec{r}_\mathrm{a}$ and $\vec{r}_\mathrm{b}$.

We now consider an *electromagnetic* field, in which case both the spatial coherence *and* polarization DOFs must be considered simultaneously. Coherence at two points $\vec{r}_\mathrm{a}$ and $\vec{r}_\mathrm{b}$ is then captured by a 4×4 Hermitian two-point vector coherency matrix [5,7]:

$$\mathbf{G} = \begin{pmatrix} G_{\mathrm{Ha,Ha}} & G_{\mathrm{Ha,Hb}} & G_{\mathrm{Ha,Va}} & G_{\mathrm{Ha,Vb}} \\ G_{\mathrm{Hb,Ha}} & G_{\mathrm{Hb,Hb}} & G_{\mathrm{Hb,Va}} & G_{\mathrm{Hb,Vb}} \\ G_{\mathrm{Va,Ha}} & G_{\mathrm{Va,Hb}} & G_{\mathrm{Va,Va}} & G_{\mathrm{Va,Vb}} \\ G_{\mathrm{Vb,Ha}} & G_{\mathrm{Vb,Hb}} & G_{\mathrm{Vb,Va}} & G_{\mathrm{Vb,Vb}} \end{pmatrix}; \quad (2)$$

here $G_{jk,j'k'} = \langle E_j(\vec{r}_k)E_{j'}^*(\vec{r}_{k'})\rangle$, $G_{jk,j'k'} = G_{j'k',jk}^*, j,j' = \mathrm{H},\mathrm{V}$, and $k,k' = \mathrm{a},\mathrm{b}$. The Hermiticity of $\mathbf{G}$ reduces the number of real parameters necessary to uniquely specify it to 16. It is critical to note that it is *not* possible to reconstruct $\mathbf{G}$ from independent polarization and spatial measurements. To observe this fact, first ignore the polarization DOF. The spatial coherence is then characterized by a *reduced* spatial coherency matrix (obtained by carrying out a partial trace over the polarization DOF in $\mathbf{G}$):

$$\mathbf{G}_\mathrm{s}^{(\mathrm{r})} = \begin{pmatrix} G_{\mathrm{Ha,Ha}} + G_{\mathrm{Va,Va}} & G_{\mathrm{Ha,Hb}} + G_{\mathrm{Va,Vb}} \\ G_{\mathrm{Hb,Ha}} + G_{\mathrm{Vb,Va}} & G_{\mathrm{Hb,Hb}} + G_{\mathrm{Vb,Vb}} \end{pmatrix}. \quad (3)$$

The polarization-independent spatial-coherence measures V and D_s may be determined from $\mathbf{G}_\mathrm{s}^{(\mathrm{r})}$. Similarly, by ignoring the spatial DOF we obtain a *reduced* polarization coherency matrix for the total field at both $\vec{r}_\mathrm{a}$ *and* $\vec{r}_\mathrm{b}$ (i.e., without spatially resolving the two points):

$$\mathbf{G}_\mathrm{p}^{(\mathrm{r})} = \begin{pmatrix} G_{\mathrm{Ha,Ha}} + G_{\mathrm{Hb,Hb}} & G_{\mathrm{Ha,Va}} + G_{\mathrm{Hb,Vb}} \\ G_{\mathrm{Va,Ha}} + G_{\mathrm{Vb,Hb}} & G_{\mathrm{Va,Va}} + G_{\mathrm{Vb,Vb}} \end{pmatrix}, \quad (4)$$

which may be used to determine D_p. By inspection, it is clear that $\mathbf{G}_\mathrm{p}^{(\mathrm{r})}$ and $\mathbf{G}_\mathrm{s}^{(\mathrm{r})}$ are insufficient to reconstruct $\mathbf{G}$. The elements of $\mathbf{G}$ that are missing from $\mathbf{G}_\mathrm{p}^{(\mathrm{r})}$ and $\mathbf{G}_\mathrm{s}^{(\mathrm{r})}$ are those that account for correlations between polarization and spatial DOFs. Determining these elements requires joint polarization–spatial measurements.

In addressing the task of completely reconstructing $\mathbf{G}$, we take inspiration from an analogous problem in quantum optics, where the polarization of two-photon states of light is encoded by a 4×4 density matrix $\hat{\rho}$ in the Hilbert space formed of the *direct product* of the Hilbert spaces that characterize the polarization of each photon [10]. An isomorphism between $\hat{\rho}$ (for the quantum state) and $\mathbf{G}$ (for the classical field) is established by identifying the vector spaces for the state of each photon in the former with the vector spaces representing the DOFs of the classical beam. That is, we identify mathematically the polarization of the *first* photon, for example, in the two-photon state with the *polarization* of the classical field. Then we identify the polarization of the *second* photon with the *spatial* DOF of the classical field.

The measurements necessary to reconstruct $\hat{\rho}$ for composite quantum systems were identified by Wootters [12] (see also Refs. [13,14]). For a quantum system comprising two subsystems, the necessary measurements to reconstruct $\hat{\rho}$ are the correlation of pairs of projective measurements, one for each subsystem, chosen from the sets of measurements that are sufficient to reconstruct the state of *each* subsystem. In other words, the measurements required to completely specify the

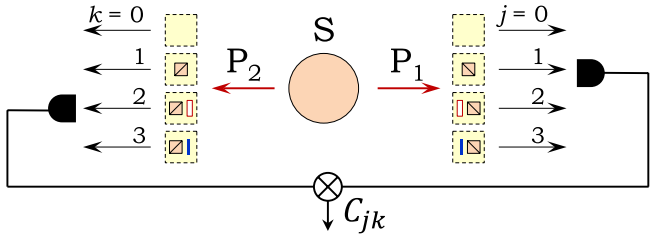

Fig. 2. Setup for measuring the two-photon polarization density matrix $\hat{\rho}$ through projective measurements on photons P_1 and P_2 emitted from a two-photon source S. C_{jk} is the probability of coincidence detection after polarization projections j and k (shown here is the particular measurement C_{12} out of 16 potential measurements). See Fig. 1 for a definition of the components.

subsystems are, surprisingly, sufficient to specify the complete system—so long as they are carried out *jointly*. Therefore, in the case of a two-photon polarization state, *each* photon is directed to the four polarization analyzers used in Fig. 1(a) [8,9]. In the two-photon measurement scheme (Fig. 2) 16 measurements are obtained by pairing polarization measurements implemented in the paths of photons traveling to the right (P_1) and left (P_2).

The isomorphism between $\hat{\rho}$ and **G** guarantees that an analogous measurement strategy is *sufficient* to uniquely reconstruct **G** for the classical beam. The required measurements to reconstruct **G** correspond to cascading pairs of $4 \times 4 = 16$ projections, one for each DOF of the classical beam. These (real) tomographic measurements that span both DOFs may then be inverted to obtain the complex elements of **G**. An arrangement where spatial measurements follow polarization projections is shown in Fig. 1(c). The order of the projective measurements may also be reversed where polarization measurements follow spatial projections. To the best of our knowledge and despite the fundamental importance of **G**, the experimental scheme we have described here for tomographically reconstructing **G** has not been realized to date.

We relate the real measurements I_{jk} to the complex elements of **G** by first defining a new set of Stokes parameters, $\mathbf{G} = (1/4)\sum_{\ell,m=0}^{3} S_{\ell m}\hat{\sigma}_{\ell}^{\mathrm{p}} \otimes \hat{\sigma}_{m}^{\mathrm{s}}$ ($\otimes$ is the direct product). The elements of **G** are then given explicitly as shown in Eq. (5). In this formulation the (real) multi-DOF Stokes parameters $S_{\ell m}$ are determined by the measurements following the relationship $S_{\ell m} = 4I_{\ell m} - 2I_{\ell 0} - 2I_{0m} + I_{00}$, ℓ, $m = 0\ldots3$. Therefore, once the multi-DOF Stokes parameters $S_{\ell m}$ are obtained, they may be substituted into

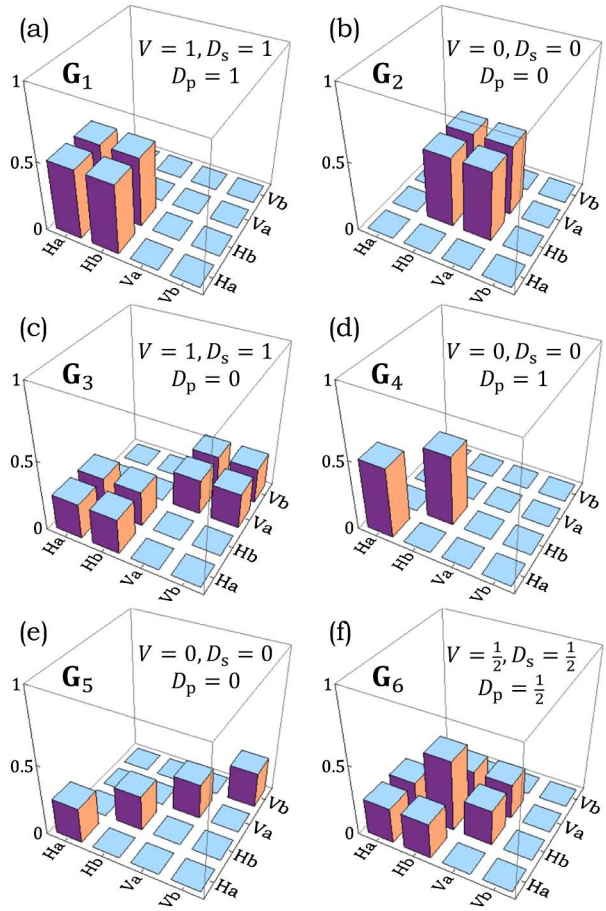

Fig. 3. (a)–(f) Pictorial depictions of the real part of the coherency matrices **G** for the fields described in the text; the imaginary parts of the elements of **G** in all these cases are zero. The labels correspond to the indices of the elements of **G** in Eq. (2).

thereby completing the inversion of the measurements and tomographic reconstruction of **G**. Thus, there is no need to carry out separate polarization measurements at $\vec{r}_{\mathrm{a}}$ or $\vec{r}_{\mathrm{b}}$. Note that if **G** is normalized to unit trace ($S_{00} = 1$), then *complete coherence* is achieved when $\mathrm{Tr}\{\mathbf{G}^2\} = 1$, and complete spatial *and* polarization incoherence occur when $\mathrm{Tr}\{\mathbf{G}^2\} = 1/4$.

Reconstructing **G** *uniquely* defines the coherence state of the field at any two points, thereby lifting ambiguities that arise from the use of only a few scalar parameters, especially when the DOFs are correlated. To highlight this crucial feature of **G**, we describe below six examples of fields where we compare V, D_{s}, or D_{p}—extracted from traditional measurements—to the information extracted from the reconstructed **G**. We present a pictorial depiction of the coherency matrices

$$\mathbf{G} = \frac{1}{4}\begin{pmatrix} S_{00}+S_{01}+S_{10}+S_{11} & S_{02}+S_{12}-i(S_{03}+S_{13}) & S_{20}+S_{21}-i(S_{30}+S_{31}) & S_{22}-S_{33}-i(S_{23}+S_{32}) \\ S_{02}+S_{12}+i(S_{03}+S_{13}) & S_{00}-S_{01}+S_{10}-S_{11} & S_{22}+S_{33}+i(S_{23}-S_{32}) & S_{20}-S_{21}-i(S_{30}-S_{31}) \\ S_{20}+S_{21}+i(S_{30}+S_{31}) & S_{22}+S_{33}-i(S_{23}-S_{32}) & S_{00}+S_{01}-S_{10}-S_{11} & S_{02}-S_{12}-i(S_{03}-S_{13}) \\ S_{22}-S_{33}+i(S_{23}+S_{32}) & S_{20}-S_{21}+i(S_{30}-S_{31}) & S_{02}-S_{12}+i(S_{03}-S_{13}) & S_{00}-S_{01}-S_{10}+S_{11} \end{pmatrix}, \quad (5)$$

in Fig. 3 that appropriates the methodology common in quantum state tomography.

(1) $\mathbf{G}_1$ corresponds to a spatially coherent, horizontally polarized field with equal amplitudes at $\vec{r}_a$ and $\vec{r}_b$, in which case $V = D_s = D_p = 1$ [Fig. 3(a)]. Here, it is clear that $\mathbf{G}_1$ separates into a direct product of the coherency matrices for the uncoupled DOFs: $\mathbf{G}_1 = \left(\begin{smallmatrix}1 & 0\\ 0 & 0\end{smallmatrix}\right)^p \otimes (1/2)\left(\begin{smallmatrix}1 & 1\\ 1 & 1\end{smallmatrix}\right)^s$. This indicates that the two DOFs are independent [as is also clear in Fig. 3(a)] and, since $\mathrm{Tr}\{\mathbf{G}^2\} = 1$, each is fully coherent.

(2) The importance of reconstructing $\mathbf{G}$ becomes apparent when examining fields in which the spatial and polarization DOFs are correlated, or *classically entangled*. Consider $\mathbf{G}_2$ that corresponds to a coherent field with orthogonal polarizations at $\vec{r}_a$ and $\vec{r}_b$ [Fig. 3(b)]. Although there is no randomness, the usual indicators of coherence applied to each DOF reveal an apparent complete lack of coherence: $V = D_s = D_p = 0$. This is in contradistinction to the fact that $\mathrm{Tr}\{\mathbf{G}_2^2\} = 1$, which confirms the global coherence of the field. Such an ambiguity is resolved by noting from Fig. 3(b) that $\mathbf{G}_2$ cannot be factorized into a direct product of polarization and spatial coherency matrices, as is the case for $\mathbf{G}_1$ above. Therefore, the apparent lack of coherence is due to the classical entanglement between the two DOFs and not due to intrinsic randomness or fluctuations [5].

(3) $\mathbf{G}_3$ shown in Fig. 3(c) corresponds to a spatially coherent field with randomized polarization: $V = D_s = 1$ and $D_p = 0$. Here, $\mathbf{G}_3 = \left(\begin{smallmatrix}1 & 0\\ 0 & 1\end{smallmatrix}\right)^p \otimes (1/2)\left(\begin{smallmatrix}1 & 1\\ 1 & 1\end{smallmatrix}\right)^s$; i.e., the two DOFs are independent and the former lacks coherence. Both features are observed clearly in Fig. 3(c).

(4) Consider the previous case of $\mathbf{G}_3$, with the role of the two DOFs reversed. In this scenario, $\mathbf{G}_4$ corresponds to a horizontally polarized field that is spatially incoherent: $V = D_s = 0$ and $D_p = 1$ [Fig. 3(d)]. Here, $\mathbf{G}_4 = \left(\begin{smallmatrix}1 & 0\\ 0 & 0\end{smallmatrix}\right)^p \otimes (1/2)\left(\begin{smallmatrix}1 & 0\\ 0 & 1\end{smallmatrix}\right)^s$; i.e., the two DOFs are independent and the latter lacks coherence. Both features are clear in Fig. 3(d), albeit with the role of polarization and space reversed with respect to Fig. 3(c).

(5) $\mathbf{G}_5$ corresponds to an unpolarized, spatially incoherent field—a maximum entropy state of the electromagnetic field [Fig. 3(e)]. In this case the field globally lacks any coherence $\mathrm{Tr}\{\mathbf{G}_5^2\} = (1/4)$, and, similarly, the reduced coherency matrices each reveal a lack of coherence ($V = D_s = D_p = 0$). By examining G as shown in Fig. 3(e), it is clear that $\mathbf{G}_5 = (1/4)\hat{\sigma}_0^p \otimes \hat{\sigma}_0^s$, corresponding to intrinsic randomness in all DOFs of the field.

(6) $\mathbf{G}_6$ corresponds to a partially coherent, partially polarized field with correlated DOFs [Fig. 3(f)]. This state arises if the polarization is randomized at one of the two points from an initially coherent polarized field. The coherence measures obtained from the reduced coherency matrices are $V = D_p = D_s = (1/2)$. The apparent lack of coherence here has two sources. First, incoherence stemming from intrinsic randomness, which is revealed by noting that $\mathrm{Tr}\{\mathbf{G}^2\} = (5/8) < 1$. Second, since $\mathbf{G}_6$ cannot be factorized into a direct product of reduced matrices, a fraction of the apparent incoherence is due to the correlation, or classical entanglement, between the DOFs.

Reconstruction of the 4×4 coherency matrix $\mathbf{G}$ therefore enables the identification of the origin of lack of coherence as determined from D_s and D_p. The lack of spatial coherence in $\mathbf{G}_4$, polarization coherence in $\mathbf{G}_3$, and both spatial and polarization coherence in $\mathbf{G}_5$ are all due to intrinsic randomness in the DOFs. On the other hand, in $\mathbf{G}_2$ the apparent absence of polarization and spatial coherence is due to coupling between the DOFs. Relying solely on separate polarization and spatial measures leads to ambiguities, which are lifted after reconstructing $\mathbf{G}$, since $\mathbf{G}$ provides a *complete* description of the field at two points. Furthermore, other parameters (such as the recently proposed Bell's measure [5]) may also be calculated from $\mathbf{G}$ and used as descriptors. Moreover, reconstructing $\mathbf{G}$ for a beam before and after transmission through a system that couples different DOFs, as in a photonic crystal or anisotropic scatterers, will help elucidate the system's characteristics.

In conclusion, we have demonstrated that the necessary measurements for characterizing the joint polarization-spatial coherence properties of an electromagnetic field are cascades of the projective measurements needed for each DOF separately. The principle of this method may be extended to other DOFs (such as optical orbital angular momentum or other spatial modes,) by using appropriate projective measurements [15,16]. This result hinges on the fact that the vector space describing the properties of an electromagnetic field having multiple DOFs[5,17] is the direct product of the vector spaces corresponding to each DOF. Consequently, multi-DOF classical beams of light may be placed in one-to-one correspondence with states of multipartite quantum systems, and quantum state tomographic strategies may thus be employed in the classical setting.

References

1. L. Mandel and E. Wolf, Rev. Mod. Phys. **37**, 231 (1965).
2. F. Gori, Opt. Lett. **23**, 241 (1998).
3. E. Wolf, Phys. Lett. A **312**, 263 (2003).
4. P. Réfrégier and F. Goudail, Opt. Express **13**, 6051 (2005).
5. K. H. Kagalwala, G. Di Giuseppe, A. F. Abouraddy, and B. E. A. Saleh, Nat. Photonics **7**, 72 (2013).
6. J. Peřina, *Coherence of Light* (Van Nostrand, 1972).
7. F. Gori, M. Santarsiero, and R. Borghi, Opt. Lett. **31**, 858 (2006).
8. D. F. V. James, P. G. Kwiat, W. J. Munro, and A. G. White, Phys. Rev. A **64**, 052312 (2001).
9. A. F. Abouraddy, A. V. Sergienko, B. E. A. Saleh, and M. C. Teich, Opt. Commun. **201**, 93 (2002).
10. U. Fano, Rev. Mod. Phys. **55**, 855 (1983).
11. W. H. McMaster, Rev. Mod. Phys. **33**, 8 (1961).
12. W. K. Wootters, *Complexity, Entropy, and the Physics of Information*, W. H. Zurek, ed. (Addison-Wesley, 1990), pp. 39–46.
13. S. Bergia, F. Cannata, A. Cornia, and R. Livi, Found. Phys. **10**, 723 (1980).
14. H. Araki, Commun. Math. Phys. **75**, 1 (1980).
15. A. F. Abouraddy, T. M. Yarnall, and B. E. A. Saleh, Opt. Lett. **36**, 4683 (2011).
16. A. F. Abouraddy, T. M. Yarnall, and B. E. A. Saleh, Opt. Lett. **37**, 2889 (2012).
17. R. J. C. Spreeuw, Found. Phys. **28**, 361 (1998).